PTTG1 Over-expression in Adrenocortical Cancer is Associated with Poor Survival and Represents a Potential Therapeutic Target

Michael J. Demeure, MD, MBA[1], **Kathryn E. Coan, MD**[2], **Clive S. Grant, MD**[3], **Richard A. Komorowski, MD**[4], **Elizabeth Stephan, PhD**[1], **Shripad Sinari, MS**[1], **David Mount, PhD**[5], and **Kimberly J. Bussey, PhD**[1]

[1]Translational Genomics Research Institute, Phoenix, AZ

[2]Mayo Clinic, Scottsdale, AZ

[3]Mayo Clinic, Rochester MN

[4]Medical College of Wisconsin, Milwaukee, WI

[5]University of Arizona Cancer Center, Tucson, AZ

Abstract

Background—Adrenocortical carcinoma (ACC) is associated with poor survival rates. The objective of the study was to analyze ACC gene expression profiling data for prognostic biomarkers and therapeutic targets.

Methods—44 ACC and 4 normal adrenals were profiled on Affymetrix U133 Plus 2 expression microarrays. Pathway and transcriptional enrichment analysis was performed. Protein levels were determined by western blot. Drug efficacy was assessed against ACC cell lines. Previously published expression datasets were analyzed for validation.

Results—Pathway enrichment analysis identified marked dysregulation of cyclin-dependent kinases and mitosis. Over-expression of PTTG1, which encodes securin, a negative regulator of p53, was identified as a marker of poor survival. Median survival for patients with tumors expressing high PTTG1 levels (log2 ratio of PTTG1 to average beta-actin <-3.04) was 1.8 years compared to 9.0 years if tumors expressed lower levels of PTTG1 (P<0.0001). Analysis of a previously published data set confirmed the association of high PTTG1 expression with a poor prognosis. Treatment of two ACC cell lines with vorinostat decreased securin levels and inhibited cell growth (IC50s of 1.69 uM and 0.891 uM, for SW-13 and H295R, respectively).

Conclusion—Over-expression of PTTG1 is correlated with poor survival in ACC. PTTG1/ securin is a prognostic biomarker and warrants investigation as a therapeutic target.

Corresponding author: Michael J. Demeure, MD, MBA 10460 N. 92nd St, Suite 401 Scottsdale AZ 85258 Telephone (480) 323-1280 Fax (480) 323-1281 mdemeure@tgen.org.

Introduction

Adrenocortical carcinoma (ACC) is an aggressive malignancy with a poor overall 5-year survival rate of 39% in patients undergoing surgical resection.[i] Complete surgical excision is the only treatment that offers the potential for a cure. Unfortunately, as many as 50% of patients have metastases at the time of diagnosis.[ii] Of those patients who undergo surgical resection, as many as 80% will develop a recurrence of their cancers.[iii] Patients with recurrent or metastatic disease have limited chemotherapeutic options. In the recently reported FIRM-ACT trial, the combination of doxorubicin, etoposide, cisplatin and mitotane yielded a response rate of only 23.2% and median survival of 14.8 months.[iv] The development of new and more effective treatments depends on an improved understanding of the molecular pathogenesis of the disease. Identification of the critical oncogenic pathways in ACC could lead to more precisely targeted and effective treatments. Previous gene expression studies have focused on identifying gene expression signatures that differentiate ACC from benign adrenal adenomas and normal adrenal tissue, and the sample sets have included both early and advanced cancers.[v,vi,vii,viii] To date, no single gene or pathway has emerged from these analyses as a key prognostic marker or therapeutic target in ACC.

In this study, we sought to identify novel potential prognostic markers and novel therapeutic targets through an analysis of the expression profiles of 44 ACC tumors. We identified dysregulation of the G2/M checkpoint of the cell cycle in ACC. Several genes involved in G2/M transition showed coordinate expression with cyclin-dependent kinase 1 (CDK1). Amongst these concordant genes, we found a strong correlation of poor survival with over-expression of pituitary tumor-transforming gene-1 (PTTG1). Targeting the PTTG1 gene product securin, with vorinostat resulted in ACC cell line growth inhibition suggesting that it is a potential therapeutic target.

Materials and Methods

Clinical Samples

A set of 44 ACC flash frozen tumors and 4 normal whole adrenal glands were collected at the Mayo Clinic in Rochester, Minnesota, the University Hospital Essen (Essen, Germany), the University of Calgary (Alberta, Canada), and Scottsdale Healthcare (Scottsdale, Arizona), as well as donated directly by patients through their community care settings. Uninvolved normal adrenal gland tissues were obtained during autopsy. Research materials were obtained under protocols approved by the Western Institutional Review Board. The diagnosis of ACC was confirmed by review of the pathology report and when necessary by an experienced endocrine pathologist (RAK) re-examining the histopathology. Stage was defined using the European Network for the Study of Adrenal Tumors Classification 2008, based on the number of mitosis per high-power field (HPF), presence or absence of necrosis, and presence or absence of atypical mitosis.[ix] Grade 1 was defined by <5 mitosis per 50 HPF, no evidence of necrosis or atypical mitosis. Grades 2-4 all had evidence of necrosis and atypical mitosis and as were distinguished by number of mitosis per HPF. Grade 2 had 5-20 mitosis per 50 HPF; grade 3, 21-50 per 50 HPF; grade 4, > 50/50 HPF. A Weiss score[x] was unavailable in previous pathology notes and was unable to be assessed prospectively

because of a limited number of available histology slides in our retrospective series. Additional pooled normal adrenal RNA was obtained commercially (BioChain Institute Inc, Newark CA).

Expression Analysis

RNA was extracted from 100 mg samples of ACC tumors and normal adrenal tissue, amplified and reverse transcribed utilizing the MessageAmp II Biotin Enhanced Kit (Ambion Life Technologies Corp, Carlsbad CA). Biotin-labeled cRNA was synthesized according to this standard protocol, followed by purification through provided cRNA Filter Cartridges. Labeled cRNA was fragmented and hybridized to Affymetrix U133 Plus 2 human genome arrays following the standard Affymetrix protocol (Affymetrix Inc., Santa Clara CA). Scanning and washing was completed on the Fluidic Stations FS450 and the GeneChip® Scanner 3000 with Workstation. Validation of the initial expression profiles was done via both hybridization to a different microarray platform and RT-qPCR. Data for ACC 30 – ACC 150 was generated from chipped samples sent to Clinical Reference Laboratory (Lenexa, KS) for RNA extraction and array processing.

Statistical Analysis

Array quality for ACC 1 – 28, MPI 1-3, and the normal samples was assessed using the Affy QCReport package in Bioconductor and the R statistical language. All arrays passed the quality controls at the site the assays were performed. All subsequent data normalization and statistical analysis was done using GenePattern (Broad Institute, www.broadinstitute.org).[xi] Expression array data was normalized by gcRMA with quantile normalization and background subtraction after using the Expression File Creator.[xii] Data was then floored at 5.5 using Preprocess Dataset, and filtered to remove 1) probes with more than 35 floored values and/or 2) probes where all values from one batch were floored while values from the other batch were not. Further batch effects were minimized using ComBat with the parametric option.[xiii] Differentially expressed genes were determined using a T-test with multiple comparison correction as implemented by Comparative Marker Selection in Gene Pattern. Genes with the corrected p-value < 0.005 and the FDR < 0.075 were selected for further study. For comparing high to low grade or primary to recurrence, the FDR cut-off was increased to < 0.13. Survival analysis was conducted using Prism 6 (GraphPad) to generate Kaplan-Meier curves that were compared by log-rank. The data discussed in this publication have been deposited in NCBI's Gene Expression Omnibus and are accessible through GEO Series accession number GSE19776 (http://www.ncbi.nlm.nih.gov/geo/query/acc.cgi?acc=GSE19776). Reviewer link: http://www.ncbi.nlm.nih.gov/geo/query/acc.cgi?token=lnkbluyayiqocto&acc=GSE19776

Integration of data with previously published data sets

Previously reported data from the expression profiling on Affymetrix U133 Plus 2 microarrays of normal adrenal glands, adrenal adenomas, and ACCs as reported by Giordano, et al.[7] was downloaded from GEO. Other datasets in the literature were not annotated with survival so they could not be used. The data was filtered to include only that from normal adrenal glands and ACCs from patients over the age of 18. Using Gene Pattern[11] this data was normalized by gcRMA[12] with quantile normalization and

background subtraction using Expression File Creator. Expression values for probes corresponding to PTTG1 and beta-actin (203554_x_at, AFFX-HSAC07/X00351_5_at, and AFFX-HSAC07/X00351_M_at) were extracted and compared to survival as above. Prism 6 was also used to calculate t-tests to compare PTTG1/beta-actin ratios between previously reported clusters as well as to compare the survival distributions between our cohort and the cohort from Giordano, et al.[7]

RT-PCR validation

Total RNA was reverse transcribed utilizing random hexamer primers and the iScript cDNA Synthesis kit (Bio-Rad Laboratories, Inc., Hercules CA). The resulting cDNA was amplified on the iQ5 Real-Time PCR Detection System (Bio-Rad Laboratories, Inc., Hercules CA) using the iScript RT-PCR Kit with SYBR green and gene specific primers designed to span the closest intron-exon junction of the reference sequence to which the probes on the array were designed (Table 1). For amplification, the following program was employed: a 50°C preheat step for 2 min., a 95°C heat activation step for 2 min., followed by 40 cycles of denaturation at 95°C for 15 sec., annealing at the appropriate temperature (Table 1) for 30 sec., and elongation at 72°C for 30 sec. Melting curve analysis was performed to evaluate primer set specificity. Beta-actin was used as the reference gene. Fold difference in cDNA concentration was calculated using the Pfaffl method taking into account reaction efficiencies.[xiv]

Pathway and transcriptional regulation analysis

Both pathway enrichment and transcriptional regulation for differentially expressed genes were analyzed using MetaCore (Thompson Reuters, New York NY). Data were analyzed by Gene Set Enrichment Analysis (www.broadinstitute.org/gsea/index.jsp)[xv] using curated gene sets corresponding to Gene Ontology categories followed by Leading Edge analysis of the enriched categories, or if that was a small number, categories with nominal p-values < 0.05, to identify genes whose expression drove enrichment.

Western blot analysis

Cells were plated in 100 mm dishes and allowed to adhere for 24 hours. Cells were then exposed to compound for 24 hours. At 24 hours, cells were lysed with RIPA buffer, and the resulting protein lysate quantitated by BCA (Thermo Fisher Scientific, Rockford IL). Thirty micrograms of protein per lane was loaded on 4-12% denaturing polyacrylamide gels, separated by gel electrophoresis, and transferred to PVDF membranes. Membranes were blocked by incubation in TBST (50 mM Tris.HCl, pH 7.4, 150 mM NaCl, 0.1% Tween 20) with 5% dry milk for 1 hour at room temperature and incubated overnight with primary antibody in TBST with 1% milk at 4°C. Membranes were washed five times in TBST for 3 minute each, and then incubated with horseradish perioxidase conjugated secondary antibody diluted 1:5,000 in 5% milk-TBST. Signal was developed using Western Lightening Plus ECL (Perkin-Elmer, Waltham MA) and visualized with Bio Spectrum 500 Imaging System with LM-26 and BioChemi 500 Camera f/1.2 P/N 97-0362-01 (UVP Cambridge UK). The primary antibodies used were securin (ab3305, Abcam, Cambridge MA) and anti-beta-actin (#4967, Cell Signaling Technology, Danvers MA). Semi-quantitative analysis was performed using Image J9 software and reported as a ratio of securin to beta-actin.

In vitro drug dose response curves

Human ACC cell lines were obtained from American Type Culture Collection (ATCC). NCI-H295R cells were plated at a density of 1750 cell/well in 40 L of DMEM/F12 with 2.5% NuSerum™ (Becton, Dickinson and Company, Franklin Lakes NJ). SW-13 cells were plated at 1250 cells/wells in 40 L DMEM with 2% FBS. Twenty-four hours after plating, serial dilutions of test compounds in 10 L of medium were added in replicates of 20 to the plates. Cells were then incubated for an additional 48, 72, 96, or 120 hours at 37°C in a humidified incubator. Viability was assessed by CellTiter-Glo® (Promega, Madison WI) and converted to normalized percent viability after normalizing to cells alone and with drug carrier, DMSO. Dose response curves and IC50 values for cell survival in the presence of the drugs were calculated using Prism5 software (graphpad.com) using the log (inhibitor) vs. response – 4 parameter function which fits the following equation: Y=Bottom + (Top-Bottom)/(1+10^(X-LogIC50)) where X is the logarithm of concentration and Y is the percent cell survival.

Results

Clinical Parameters

Forty-four adrenocortical cancers were included in our analysis (Table 2). These samples were obtained from 27 women and 16 men with a median age of 52.5 years (range 20 to 72.1) and included a primary and metastasis pair from one female patient. The median size of the tumors was 9.25 cm (2.5 cm – 19 cm), and the median weight of the tumors was 230 g (22 g – 2310 g). The median survival of the patients was 3.05 years (0 – 18 years).

Expression Analysis

Differential gene expression analysis revealed that 1843 probes representing 1485 genes were differentially expressed between ACC and normal. The top 50 over- and under-expressed probes, along with the log2 fold-change are given in Table 3. Pathway enrichment analysis demonstrated that there dysregulation in G2/M transition was enriched in ACC (Figure 1). This dysregulation focused on the sister chromatid adhesion and homologous recombination DNA repair. To determine whether the G2/M signature that we observed in the ACC samples was overwhelming our ability to detect other pathways, we used the 70 gene signature of chromosomal instability (CIN70)[xvi] as a proxy, removed these genes from the data, and re-ran our analysis. The results from these analyses indicated that while normal adrenal tissue is enriched for both IGF1R and EGFR signaling, ACCs continue to retain evidence of cell cycle perturbations that become more pronounced with increasing tumor grade (Figure 2).

Metacore was used to examine the data for evidence of specific transcription factor involvement. We determined that Sp1, HNF4α, p53, and c-myc play a role in the transcriptional program of ACC. In particular, we observed that the majority of genes repressed by p53 are over-expressed, while expression genes enhanced by p53 are reduced in ACC samples (Figure 3). Most genes that are targets of HNF4α are increased in their expression, while targets of Sp1 are primarily repressed. Targets of c-myc are dysregulated but not in an obviously coherent fashion.

Survival analysis

Our analysis identified perturbations of the p53 pathway and significant dysregulation of the G2/M transition. Subsequently, we decided to examine genes showing coordinate expression with CDK1/p34, the primary cyclin-dependent kinase of the G2/M transition, for association with survival. We identified PTTG1 as showing coordinate expression with CDK1 and found over-expression to inversely correlate with survival (Figure 4). Median survival for patients with tumors expressing high PTTG1 levels (log2 value of PTTG1 to average beta-actin > −3.04) was 1.83 years compared to 9.0 years if tumors expressed lower levels (p<0.0001). This association was replicated in our analysis of the Giordano dataset (Figure 5).[7] While the difference in survival is not significant (Figure 5A), we observed that the mean expression of PTTG1 did differ significantly based on cluster membership which the authors reported had a survival difference (Figure 5B). This suggested that the signal in this data set was attenuated. Looking at the survival data, it became clear that the cohort of patients analyzed lacked long-term survivors, thus explaining the results (Figure 5C). When we analyzed the two data sets together, the significant correlation with survival remained (p=0.004, Figure 5D).

Pathway-based treatment studies

Several chemotherapeutic agents target proteins involved in the G2/M transition. The lack of association between the proteins involved in the G2/M transition with either aneuploidy or cell cycle perturbations in our data suggested to us the possibility that the up-regulation of the G2/M pathway was indicative of vulnerability in the pathway. To investigate whether PTTG1/securin could represent a novel therapeutic target, we treated two ACC cell lines, SW-13 and H295R, with the histone deacytlase inhibitor, vorinostat, which has previously been shown to decrease PTTG1 expression and securin levels in colorectal cells.[xvii] Vorinostat inhibited cell growth with IC50 values of 1.69 M and 0.891 M, for SW-13 and H295R, respectively. Vorinostat also resulted in a concentration dependent decrease in securin protein levels in both cell lines (Figure 6).

Discussion

In this study of 44 ACC tumors, we implicate aberrations in the p53 pathway and dysregulation of cell cycle progression though G2/M to be involved in the pathogenesis of ACC. We examined genes showing coordinate expression with the primary cyclin-dependent kinase of the G2/M transition, CDK1/p34, for interaction with p53 and association with survival. PTTG1 was coordinately expressed with CDK1. Over-expression of PTTG1 was observed in 84 % of ACC samples and was significantly associated with poor survival (P <0.0001). We applied our analysis to the previously published data of Giordano, et al.[7] treating this data as a validation set. When we combined our data with that of the Giordano set, our findings remained. Due to the absence of annotation with survival information, our findings linking PTTG1 to survival could not be verified by analysis of other published datasets including that of deReynies et al.[6] PTTG1 over-expression has been reported in multiple tumor types including those of the pituitary, breast, thyroid, ovarian, uterine, colon, and lung,[xviii] and has been associated with increased invasion and vascularity.[xix] It has also been implicated as a "signature gene" for metastatic disease.[xx]

PTTG1 encodes the protein securin. Securin suppresses both the transcriptional activity of p53 and p53 mediated apoptosis.[xxi] Securin is involved in G2M transition, regulating the transition into M-phase and sister chromatid separation.[xxii] Securin is also involved in the nonhomologous end-joining DNA repair pathway.[22] PTTG1 also interacts with both Sp1, and c-myc, two of the other specific transcription factors identified by our analysis to be involved in ACC pathogenesis. PTTG1 and Sp1 act coordinately to increase cyclin D and promote G1/S phase transition independent of p21.[xxiii] Sp1 also binds a PTTG1 promotor sequence thereby regulating PTTG1 expression.[23] Furthermore, PTTG1 serves as transcription activator of the c-myc oncogene.[xxiv] Taken together, these findings suggest how PPTG1 expression may influence ACC progression.

In order to study whether targeting PTTG1/securin could have therapeutic efficacy, we used the vorinostat, a histone deacetylase, HDAC, inhibitor, vorinostat. We chose a HDAC inhibitor because they have been shown to decrease PTTG1 gene expression and securin protein levels in colorectal cell lines.[17] Vorinostat is currently approved to treat cutaneous T-cell lymphoma thus making it an attractive agent for rapid clinical translation. Treating two ACC cell lines with vorinostat decreased securin levels and inhibited cell growth. PTTG1/securin has been targeted, *in vitro* and *in vivo,* with short interfering RNA (si-RNA) with resulting inhibition of tumor growth.[xxv] Because of the indirect mechanism of action of vorinostat on securin levels, we cannot rule out additional contributions of HDAC inhibition to the observed loss in viability. Nevertheless, our findings suggest that drugs targeting PTTG1/securin should be investigated for a potential therapeutic utility in ACC.

In summary, our expression profiling analyses in ACC have identified the G2/M transition and in particular, sister chromatid adhesion and separation, as perturbed in ACC. The finding of p53 transcriptional enrichment highlights the importance of this pathway in ACC. Increased expression of *PTTG1*, which plays a role in both sister chromatid adhesion and p53 regulation, was associated with poor prognosis in our samples. Taken together, these results suggest ACC pathogenesis is driven in part by deficiencies in p53 pathway function, with vulnerabilities in the G2/M transition that may expose viable therapeutic targets, including potentially PTTG1. Further investigation into the role PTTG1 over-expression in the pathogenesis of ACC and validation of PTTG1/securin as a prognostic marker or potential therapeutic target is warranted.

Acknowledgments

References

i. Bilimoria KY, Shen WT, Elaraj D, Bentrem DJ, Winchester DJ, Kebebew E, et al. Adrenocortical carcinoma in the United States: treatment utilization and prognostic factors. Cancer. 2008; 113:3130–6. [PubMed: 18973179]

ii. Demeure MJ, Somberg LB. Functioning and nonfunctioning adrenocortical carcinoma. Surg Oncol Clin North Am. 1998; 7:791–805.

iii. Terzolo M, Berruti A. Adjunctive treatment of adrenocortical carcinoma. Curr Opin Endocrrinol Diabetes Obes. 2008; 15:221–6.

iv. Fassnacht M, Terzolo M, Allolio B, Baudin E, Haak H, Berruti A, et al. Combination chemotherapy in advanced adrenocortical carcinoma. N Engl J Med. 2012; 366:2189–97. [PubMed: 22551107]

v. de Fraipont F, El Atifi M, Cherradi N, Le Moigne G, Defaye G, Houlgatte R, et al. Gene expression profiling of human adrenocortical tumors using complementary deoxyribonucleic Acid microarrays identifies several candidate genes as markers of malignancy. J Clin Endocrinol Metab. 2005; 90:1819–29. [PubMed: 15613424]

vi. de Reyniès A, Assie G, Rickman DS, Tissier F, Groussin L, Rene-Corail F, et al. Gene expression profiling reveals a new classification of adrenocortical tumors and identifies molecular predictors of malignancy and survival. J Clin Oncol. 2009; 27:1108–15. [PubMed: 19139432]

vii. Giordano TJ, Kuick R, Else T, Gauger PG, Vinco M, Bauersfeld J, et al. Molecular classification and prognostication of adrenocortical tumors by transcriptome profiling. Clin Cancer Res. 2009; 15:668–76. [PubMed: 19147773]

viii. Velazquez-Fernandez D, Laurell C, Geli J, Hoog A, Odeberg J, Kjellman M, et al. Expression profiling of adrenocortical neoplasms suggests a molecular signature of malignancy. Surgery. 2005; 138:1087–94. [PubMed: 16360395]

ix. Fassnacht M, Johanssen S, Quinkler M, Bucsky P, Willenberg HS, Beuschlein F, et al. Limited prognostic value of the 2004 International Union Against Cancer staging classification for adrenocortical carcinoma: proposal for a Revised TNM Classification. Cancer. 2009; 115:243–50. [PubMed: 19025987]

x. Weiss LM. Comparative histologic study of 43 metastasizing and nonmetastasizing adrenocortical tumors. Am J Surg Pathol. 1984; 8:163–9. [PubMed: 6703192]

xi. Reich M, Liefeld T, Gould J, Lerner J, Tamayo P, Mesirov JP. GenePattern 2.0. Nat Genet. 2006; 38:500–1. [PubMed: 16642009]

xii. Irizarry RA, Hobbs B, Collin F, Beazer-Barclay YD, Antonellis KJ, Scherf U, et al. Exploration, normalization, and summaries of high density oligonucleotide array probe level data. Biostatistics. 2003; 4:249–64. [PubMed: 12925520]

xiii. Johnson WE, Li C, Rabinovic A. Adjusting batch effects in microarray expression data using empirical Bayes methods. Biostatistics. 2007; 8:118–27. [PubMed: 16632515]

xiv. Pfaffl MW. A new mathematical model for relative quantification in real-time RT-PCR. Nucleic Acids Res. 2001; 29:e45. [PubMed: 11328886]

xv. Subramanian A, Tamayo P, Mootha VK, Mukherjee S, Ebert BL, Gillette MA, et al. Gene set enrichment analysis: a knowledge-based approach for interpreting genome-wide expression profiles. Proc Natl Acad Sci U S A. 2005; 102:15545–50. [PubMed: 16199517]

xvi. Carter SL, Eklund AC, Kohane IS, Harris LN, Szallasi Z. A signature of chromosomal instability inferred from gene expression profiles predicts clinical outcome in multiple human cancers. Nat Genet. 2006; 38:1043–8. [PubMed: 16921376]

xvii. Hernandez A, Lopez-Lluch G, Navas P, Pintor-Toro JA. HDAC and Hsp90 inhibitors down-regulate PTTG1/securin but do not induce aneuploidy. Genes Chromosomes Cancer. 2009; 48:194–201. [PubMed: 19006077]

xviii. Tong Y, Eigler T. Transcriptional targets for pituitary tumor-transforming gene-1. J Mol Endocrinol. 2009; 43:179–85. [PubMed: 19433493]

xix. Heaney AP, Singson R, McCabe CJ, Nelson V, Nakashima M, Melmed S. Expression of pituitary-tumour transforming gene in colorectal tumours. Lancet. 2000; 355:716–9. [PubMed: 10703804]

xx. Heaney AP, Singson R, McCabe CJ, Nelson V, Nakashima M, Melmed S. Expression of pituitary-tumour transforming gene in colorectal tumours. Lancet. 2000; 355:716–9. [PubMed: 10703804]

xxi. Bernal JA, Luna R, Espina A, Lazaro I, Ramos-Morales F, Romero F, et al. Human securin interacts with p53 and modulates p53-mediated transcriptional activity and apoptosis. Nat Genet. 2002; 32:306–11. [PubMed: 12355087]

xxii. Bernal JA, Roche M, Mendez-Vidal C, Espina A, Tortolero M, Pintor-Toro JA. Proliferative potential after DNA damage and non-homologous end joining are affected by loss of securin. Cell Death Differ. 2008; 15:202–12. [PubMed: 17962814]

xxiii. Tong Y, Tan Y, Zhou C, Melmed S. Pituitary tumor transforming gene interacts with Sp1 to modulate G1/S cell phase transition. Oncogene. 2007; 26:5596–605. [PubMed: 17353909]

xxiv. Pei L. Identification of c-myc as a down-stream target for pituitary tumor-transforming gene. J Biol Chem. 2001; 276:8484–91. [PubMed: 11115508]

xxv. Cho-Rok J, Yoo J, Jang YJ, Kim S, Chu IS, Yeom YI, et al. Adenovirus-mediated transfer of siRNA against PTTG1 inhibits liver cancer cell growth in vitro and in vivo. Hepatology. 2006; 43:1042–52. [PubMed: 16628636]

Enrichment by Pathway Maps

#	Maps	Total	In Data	Genes from Active Data
1	Cell cycle_Role of APC in cell cycle regulation	32	9	Nek2A, Tome-1, CDC20, SKP2, Cyclin B, MAD2a, Securin, CDK1 (p34), BUBR1
2	Cell cycle_The metaphase checkpoint	36	8	Nek2A, HP1 alpha, Rod, HEC, CDC20, HZwint-1, MAD2a, BUBR1
3	Cell cycle_Spindle assembly and chromosome separation	33	7	Nek2A, HEC, CDC20, Cyclin B, MAD2a, Securin, CDK1 (p34)
4	Cell cycle_Role of Nek in cell cycle regulation	32	6	Nek2A, NEK6, Cyclin B1, HEC, MAD2a, CDK1 (p34)
5	Nicotine signaling in chromaffin cells	46	6	TY3H, PNMT, DBH, Chromogranin A, nAChR alpha-3, Calmodulin
6	IL-6 signaling in colorectal cancer	37	5	Cyclin B1, Cyclin E, TGF-beta receptor type II, Cyclin B, CDK1 (p34)
7	Immune response_PGE2 signaling in immune response	45	5	HGF, NF-AT1(NFATC2), CREM (activators), CREM (repressors), SLC21A2
8	Cell cycle_Nucleocytoplasmic transport of CDK/Cyclins	14	3	Cyclin B1, Cyclin E, CDK1 (p34)
9	Cell cycle_Role of SCF complex in cell cycle regulation	29	4	Cyclin E, Skp2/TrCP/FBXW, SKP2, CDK1 (p34)
10	Angiogenesis in HCC	50	5	Epo receptor, ID1, VEGFR-1, TGF-beta receptor type II, Securin

Figure 1.
The top 10 pathway maps enriched for differentially expressed genes between ACC and normal center on cell cycle control, particularly the G2/M transition.

Enrichment by Process Networks

#	Networks	Total	In Data	Genes from Active Data
1	Cell cycle_Core	115	16	Nek2A, HP1 alpha, Cyclin B1, Rod, p57, Cyclin E, HEC, MCM7, CDC20, Cyclin B, Cyclin B2, MAD2a, Securin, CDK1 (p34), MCM5, BUBR1
2	Cell cycle_Mitosis	179	19	Nek2A, HGF, MCAK, HP1 alpha, Cyclin B1, Rod, Dynamin-2, CDC23, HEC, HP1, CDC20, HZwint-1, Cyclin B, Cyclin B2, MAD2a, Securin, CDK1 (p34), BUBR1, Dynamin
3	Cell cycle_G2-M	206	19	Nek2A, PDGF receptor, Cyclin B1, CDC23, HNF4-alpha, p38delta (MAPK13), RGC32, Skp2/TrCP/FBXW, p38 MAPK, CDC20, SKP2, Cyclin B, Cyclin B2, MAD2a, Securin, PDGF-R-alpha, CDK1 (p34), BUBR1, Dynamin
4	Cytoskeleton_Spindle microtubules	109	13	Nek2A, MCAK, Cyclin B1, Rod, HEC, CDC20, HZwint-1, Cyclin B, Cyclin B2, MAD2a, Securin, CDK1 (p34), BUBR1
5	Signal transduction_Neuropeptide signaling pathways	155	14	NPY, PC2 (SPC2), MC1R, Somatostatin, Carboxypeptidase H, Galpha(i)-specific peptide GPCRs, PACAP receptor 1, Secretogranin V, NPY1R, Enkephalin A, Galpha(q)-specific peptide GPCRs, Calmodulin, Galpha(s)-specific peptide GPCRs, CART
6	Cell adhesion_Synaptic contact	184	15	K(+) channel, subfamily J, Neurexin beta, Synaptotagmin XI, CaMK II beta, Neurexin alpha, Synaptotagmin, CNTN1 (F3), Dynamin-2, Rab-27A, Semaphorin 4C, Neurotractin, Alpha-actinin, L1CAM, Neurofascin, Alpha-actinin 1
7	Cytoskeleton_Intermediate filaments	81	9	Plakophilin 2, Keratin 8, Nestin, Keratin 6A, Alpha-actinin, TMPOA, Alpha-actinin 1, CDK1 (p34), TMPOB
8	Cell cycle_S phase	149	12	Nek2A, HP1 alpha, Cyclin B1, RGC32, Cyclin E, HP1, MCM7, Cyclin B, Cyclin B2, Securin, CDK1 (p34), MCM5
9	Reproduction_Progesterone signaling	213	15	HGF, HSD3B2, PLA2, HOXA5, Cyclin B1, HSD11B1, ADAM-TS1, HPGD, HSD3B1, CDC20, Galpha(q)-specific peptide GPCRs, Cyclin B2, MAD2a, Calmodulin, CDK1 (p34)
10	Signal transduction_CREM pathway	98	9	TY3H, DBH, PLAT (TPA), Rab-27A, ACT, NF-AT, CREM (activators), CREM (repressors), CDK1 (p34)

Figure 2.
Various aspects of cell cycle control dominate the top 10 maps enriched for differentially expressed genes between high (grades 3 and 4) and low grade (grades 1 and 2) ACC.
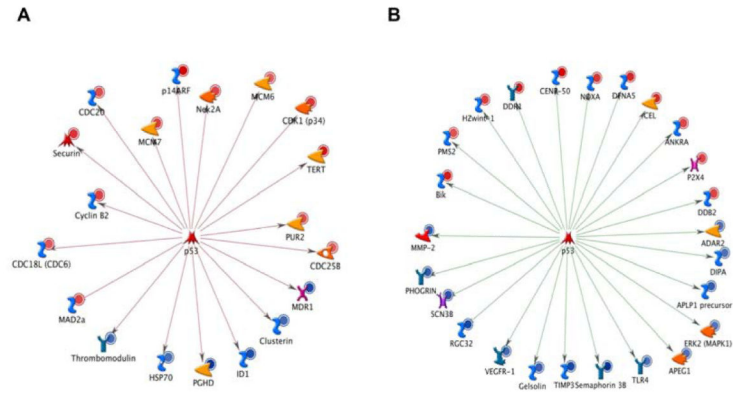
Figure 3.
p53 regulation of differentially expressed genes in ACC is aberrant. Genes that should be negatively regulated by p53, as indicated by the red arrows, are predominantly over-expressed, indicated by red circles as adjacent to the gene names. Blue circles indicate appropriate under-expression(A). Genes that should be positively regulated by p53, indicated by the green arrows, are often under-expressed as indicated by the blue circles next to the gene name (B).
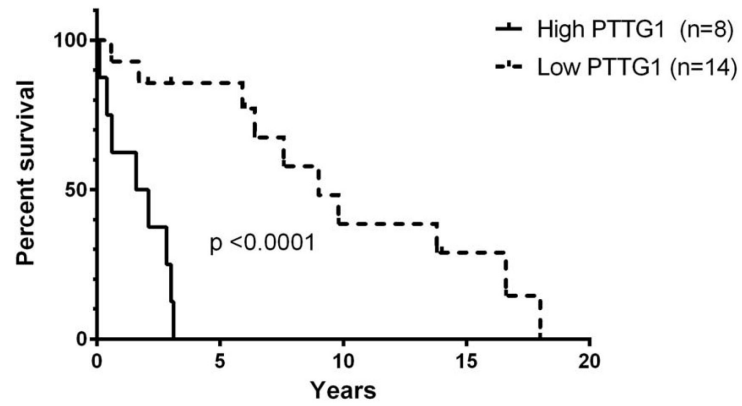
Figure 4.
Expression of high levels of PTTG1 is associated with poor survival in ACC. Hazard ratio by logrank was 3.38 (confidence interval 2.26-13.11)
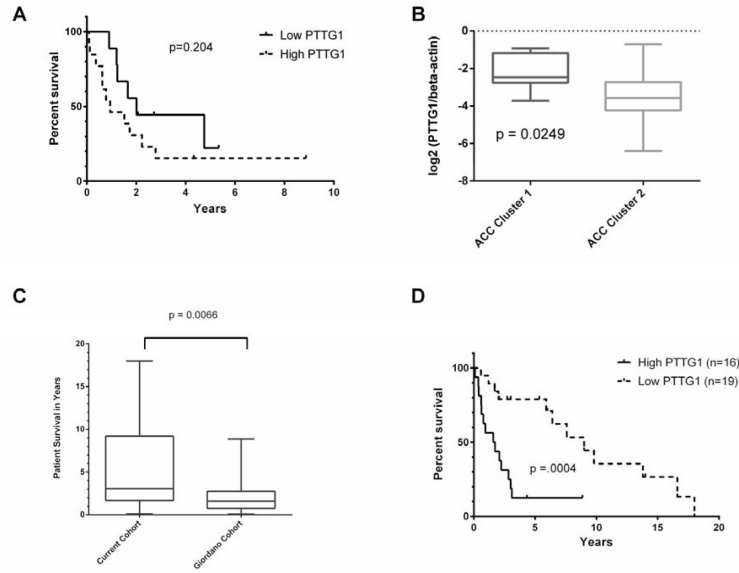
Figure 5.
Expression of high levels of PTTG1 is associated with poor survival in the data from Giordano et al.[7] A and B) Kaplan Meier analysis of survival based on PTTG1 expression was not different (p=0.204, hazard ratio by logrank was 1.87, 95% confidence interval 0.72-4.82). However, the authors did identify two cohorts of patients having differences in survival based on gene expression analysis. The mean expression level of PTTG1 was significantly higher in the cluster exhibiting poor survival (student's t-test, p = 0.0249). C) The cohort of patients presented in this report have significantly better survival that that of the cohort of patients of Giordano, et al., with the Giordano cohort having fewer long-term survivors, possibly due to the referral nature of this center's practice. D) Combining the data from both cohorts demonstrates a significant association of PTTG1 levels with survival. Hazard ratio by logrank was 3.38 (95% confidence interval 2.26-13.11)
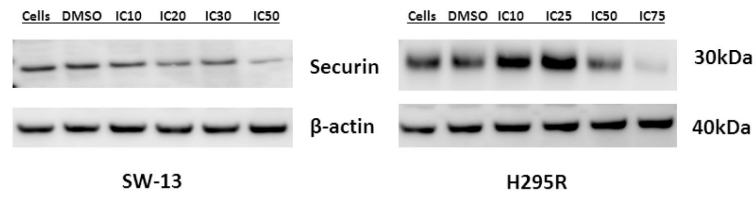
Figure 6.
Exposure of ACC cell lines to vorinostat results in a reduction in the levels of securin
protein. The ACC cell lines, SW-13 and H295R were exposed to concentrations of
vorinostat that resulted in the inhibition of growth of the percentage of cells indicated.
Securin levels decreased as the concentration of vorinostat increased.

Gene	Reference Sequence	Forward	Reverse	Annealing Temperature (°C)
E2F1	NM_005225	TGC TCT CCG AGG ACA CTG ACA GCC A	GGA GGG GCT TTG ATC ACC ATA ACC A	59
SPARC	NM_003118	TCT GAC TGA GAA GCA GAA GCT GCG G	CCG AAC TGC CAG TGT ACA GGG AAG A	62
CDC2	NM_001786	CAG GAA GCC TAG CAT CCC ATG TC	CCA GAA ATT CGT TTG GCT GGA TC	59
BIRC5	NM_001168	CCC TTG GTG AAT TTT TGA AAC TGG A	GCA CTT TCT CCG CAG TTT CCT CAA A	59
TOP2A	NM_001067	TCC TCC CCT CTG AAT TTA GTT TGG G	AAA CAA TGC CCA TGA GAT GGT CAC T	62
IGF2	NM_000612	CCA AGT CCG AGA GGG ACG TGT CGA	TGG AAG AAC TTG CCC ACG GGG	59
IGF1R	NM_000875	CCA ACG AGC AAG TCC TTC GCT TCG	GGG TTA TAC TGC CAG CAC ATG CGC	59

Sample[*]	Gender	Age (years)	Survival (years)	Tumor Size (cm)	Tumor Weight (g)	Tumor Stage	Tumor Grade
ACC 4	F	56.7	5.9	NA	NA	Recurrence	NA
ACC 5[*]	F	23.3	3.0	19	1100	2	3
ACC 8[*]	F	56.5	0.6	9	190	4	4
ACC 9[*]	M	53.2	9.0	8	195	3	2
ACC 10[*]	M	67.8	1.7	7.6	150	2	4
ACC 11[*]	F	54.2	18	15	890	2	1
ACC 12[*]	M	72.1	0.4	9.5	175	4	4
ACC 13[*]	M	46.9	0.1	12	235	4	4
ACC 17[*]	F	26.7	16.6	3	NA	Recurrence	4
ACC 19[*]	M	48.5	3.1	9	195	2	3
ACC 21[*]	F	36.9	13.8	6.5	NA	Recurrence	4
ACC 22[*]	F	67.3	6.4	10	230	2	2
ACC 23[*]	F	27.7	9.8	8	149	2	2
ACC 26[*]	F	NA	NA	NA	NA	2	3
ACC 27[*]	M	NA	NA	NA	NA	Recurrence	2
ACC 28[*]	F	58	NA	9	153.8	1	2
MPI1	M	42.0	14[+]	NA	NA	Recurrence	NA
MPI2	F	46.0	NA	NA	NA	NA	NA
MPI3[*]	F	37.0	NA	NA	NA	3	2
ACC 30	F	20	NA	18	NA	NA	1
ACC 31	F	68	1.583	NA	NA	Recurrence	2
ACC 32	F	45	NA	NA	NA	Recurrence	NA
ACC 35	M	46	NA	16.0	1463	4	NA
ACC 45	F	32	NA	11	106	2	1
ACC 47	M	43	NA	4	60	Recurrence	1
ACC 48	F	45	NA	NA	NA	4	NA
ACC 51	M	40	NA	12	480	NA	2
ACC 59	M	52	NA	19.0	2310	NA	NA
ACC 61	F	60	NA	8.8	392	3	NA
ACC 84	F	27	NA	9.5	300	NA	1
ACC 85	M	70	NA	9.0	272	NA	1
ACC 112	F	53	NA	NA	NA	4	NA
ACC 114	F	NA	NA	NA	NA	Recurrence	NA
ACC 115	F	58	NA	NA	NA	Recurrence	NA
ACC 117	M	57	3[+]	4.0	39	1	1

Sample[*]	Gender	Age (years)	Survival (years)	Tumor Size (cm)	Tumor Weight (g)	Tumor Stage	Tumor Grade
ACC 118	M	59	7.583	2.5	NA	Recurrence	NA
ACC 123	F	59	NA	10	22	4	NA
ACC 129	F	55	0.583	10.5	277	2	4
ACC 132	F	51	6[+]	14.5	325	Recurrence	2
ACC 134	F	53	2.083	14.5	1243	Recurrence	NA
ACC 136	M	69	2.83	7.8	NA	Recurrence	NA
ACC 140	M	63	2.08[+]	7.8	132	4	4
ACC 149	F	28	NA	NA	NA	4	NA
ACC 150	NA	NA	NA	NA	NA	Liver Metastasis from ACC 149	NA

[*] Sample previously reported in Stephan, et al, 2008

[+] Alive at last follow-up

NA - not available

Probe ID	Gene	Score	P-value	FDR	Fold-change	Direction
207169_x_at	DDR1	10.24	0.002	0.052	11.47	ACC
203677_s_at	TARBP2	10.01	0.002	0.052	4.64	ACC
242108_at		9.93	0.002	0.052	10.56	ACC
232135_at	SAP30L	9.93	0.002	0.052	4.27	ACC
218389_s_at	APH1A	9.76	0.002	0.052	1.77	ACC
214163_at	HSPB11	9.71	0.002	0.052	3.67	ACC
225191_at	CIRBP	9.36	0.002	0.052	26.62	ACC
55872_at	ZNF512B	9.33	0.002	0.052	4.47	ACC
239516_at		9.32	0.002	0.052	5.36	ACC
1556821_x_at	DLEU2	9.28	0.002	0.052	8.09	ACC
212913_at	MSH5	9.26	0.002	0.052	7.66	ACC
212849_at	AXIN1	9.26	0.002	0.052	1.67	ACC
91952_at	DCAF15	9.25	0.002	0.052	3.76	ACC
202253_s_at	DNM2	9.09	0.002	0.052	4.02	ACC
226072_at	FUK	9.00	0.002	0.052	2.64	ACC
227670_at	ZNF75A	8.98	0.002	0.052	3.57	ACC
209675_s_at	HNRNPUL1	8.97	0.004	0.068	2.12	ACC
1555575_a_at	KDELR1	8.94	0.002	0.052	1.74	ACC
218494_s_at	SLC2A4RG	8.93	0.002	0.052	7.85	ACC
235984_at		8.87	0.002	0.052	5.34	ACC
212194_s_at	TM9SF4	8.85	0.002	0.052	7.38	ACC
227129_x_at	FLJ45340	8.84	0.002	0.052	3.55	ACC
219818_s_at	GPATCH1	8.83	0.002	0.052	2.28	ACC
202496_at	EDC4	8.80	0.002	0.052	2.08	ACC
222843_at	FIGNL1	8.78	0.002	0.052	6.15	ACC
230142_s_at	CIRBP	8.77	0.002	0.052	15.08	ACC
224982_at	AKT1S1	8.73	0.002	0.052	2.10	ACC
228392_at	ZNF302	8.70	0.002	0.052	10.59	ACC
1557558_s_at	LOC100129196	8.66	0.002	0.052	1.83	ACC
242563_at		8.66	0.002	0.052	2.62	ACC
224709_s_at	CDC42SE2	8.63	0.002	0.052	2.40	ACC
228138_at	ZNF498	8.60	0.002	0.052	3.01	ACC
221818_at	INTS5	8.58	0.004	0.068	1.60	ACC
219947_at	CLEC4A	8.55	0.002	0.052	2.62	ACC
229473_at	MAMDC4	8.54	0.002	0.052	23.81	ACC
223589_at	ZNF416	8.51	0.002	0.052	2.04	ACC
227413_at	UBLCP1	8.50	0.002	0.052	1.83	ACC
224639_at	SPPL3	8.49	0.002	0.052	2.47	ACC
214550_s_at	TNPO3	8.46	0.002	0.052	2.82	ACC
202892_at	CDC23	8.43	0.002	0.052	2.93	ACC
224687_at	ANKIB1	8.41	0.002	0.052	1.73	ACC

Probe ID	Gene	Score	P-value	FDR	Fold-change	Direction
225899_x_at	FLJ45445	8.38	0.002	0.052	3.93	ACC
208779_x_at	DDR1	8.37	0.002	0.052	4.56	ACC
235241_at	SLC38A9	8.29	0.002	0.052	5.12	ACC
232810_at	AIG1	8.29	0.002	0.052	2.18	ACC
206854_s_at	MAP3K7	8.26	0.002	0.052	1.79	ACC
202726_at	LIG1	8.23	0.002	0.052	3.73	ACC
39313_at	WNK1	8.23	0.002	0.052	2.98	ACC
238775_at		8.20	0.002	0.052	2.87	ACC
239264_at		8.15	0.002	0.052	2.89	ACC
220795_s_at	BEGAIN	−7.25	0.002	0.052	2.37	Normal
208991_at	STAT3	−7.32	0.002	0.052	1.82	Normal
231773_at	ANGPTL1	−7.39	0.004	0.068	3.91	Normal
202359_s_at	SNX19	−7.42	0.002	0.052	1.72	Normal
225029_at	LOC550643	−7.47	0.004	0.068	1.61	Normal
221885_at	DENND2A	−7.53	0.004	0.068	1.39	Normal
224281_s_at	NGRN	−7.55	0.002	0.052	1.71	Normal
209612_s_at	ADH1B	−7.58	0.002	0.052	4.90	Normal
223582_at	GPR98	−7.67	0.002	0.052	7.42	Normal
224997_x_at	H19	−7.74	0.002	0.052	5.38	Normal
224710_at	RAB34	−7.89	0.004	0.068	3.42	Normal
206050_s_at	RNH1	−7.89	0.002	0.052	1.82	Normal
224061_at	INMT	−8.05	0.002	0.052	7.80	Normal
200059_s_at	RHOA	−8.17	0.002	0.052	1.56	Normal
202524_s_at	SPOCK2	−8.17	0.002	0.052	3.33	Normal
225185_at	MRAS	−8.22	0.002	0.052	3.62	Normal
211959_at	IGFBP5	−8.28	0.002	0.052	5.16	Normal
200006_at	PARK7	−8.29	0.002	0.052	1.38	Normal
209960_at	HGF	−8.32	0.002	0.052	5.05	Normal
214610_at	CYP11B1	−8.43	0.002	0.052	3.16	Normal
202291_s_at	MGP	−8.61	0.002	0.052	3.63	Normal
201601_x_at	IFITM1	−8.69	0.002	0.052	3.17	Normal
203088_at	FBLN5	−8.78	0.002	0.052	3.74	Normal
214091_s_at	GPX3	−8.85	0.002	0.052	5.14	Normal
212203_x_at	IFITM3	−8.85	0.002	0.052	2.14	Normal
210058_at	MAPK13	−8.95	0.002	0.052	2.87	Normal
221622_s_at	TMEM126B	−8.97	0.002	0.052	1.66	Normal
37022_at	PRELP	−8.98	0.002	0.052	3.26	Normal
226224_at	FOXK2	−9.05	0.002	0.052	2.31	Normal
201315_x_at	IFITM2	−9.13	0.002	0.052	2.61	Normal
206294_at	HSD3B2	−9.18	0.002	0.052	4.55	Normal
217845_x_at	HIGD1A	−9.20	0.002	0.052	2.05	Normal
202224_at	CRK	−9.20	0.002	0.052	1.75	Normal

Probe ID	Gene	Score	P-value	FDR	Fold-change	Direction
203225_s_at	RFK	−9.22	0.002	0.052	1.83	Normal
212361_s_at	ATP2A2	−9.25	0.002	0.052	2.24	Normal
201445_at	CNN3	−9.77	0.002	0.052	2.11	Normal
205952_at	KCNK3	−9.89	0.002	0.052	2.70	Normal
225987_at	STEAP4	−10.04	0.002	0.052	5.61	Normal
218706_s_at	GRAMD3	−10.20	0.002	0.052	2.66	Normal
225148_at	RPS19BP1	−10.25	0.002	0.052	2.61	Normal
203650_at	PROCR	−10.61	0.002	0.052	2.77	Normal
221486_at	ENSA	−10.97	0.002	0.052	1.81	Normal
225809_at	PARM1	−11.82	0.002	0.052	5.99	Normal
239451_at		−13.35	0.002	0.052	4.12	Normal
227654_at	FAM65C	−13.36	0.002	0.052	4.64	Normal
61297_at	CASKIN2	−13.73	0.002	0.052	2.00	Normal
209505_at	NR2F1	−13.78	0.002	0.052	3.89	Normal
212103_at	KPNA6	−14.60	0.002	0.052	1.74	Normal
201348_at	GPX3	−15.03	0.002	0.052	5.23	Normal
236677_at	NGB	−19.10	0.002	0.052	6.46	Normal